Interplay of Weak Interactions: An Iridium(III) System with an Agostic *tert*-Butyl but a Nonagostic Isopropyl Group

Eric Clot,[†] Odile Eisenstein,*[,†] Tiffany Dubé,[‡] Jack W. Faller,*[,‡] and Robert H. Crabtree*[,‡]

Laboratoire de Structure et Dynamique des Systèmes Moléculaires et Solides (UMR 5636), Université Montpellier 2, 34095 Montpellier Cedex 5, France, and Department of Chemistry, Yale University, 225 Prospect Street, New Haven, Connecticut 06520-8107

Received September 6, 2001

The solid state structure and NMR data of 2-substituted benzoquinoline Ir(III) complexes show that the pendant group G does not necessarily become agostic despite the presence of an available nearby coordination site at the Ir center. Thus for G = *t*-Bu the agostic structure is observed, but for G = *i*-Pr, the potentially agostic *i*-Pr methyl groups point away from the metal. ONIOM(B3PW91/UFF) calculations reproduce the experimental observations and suggest that several ligand−ligand interactions (parallel aromatic stacking and C−H···H−Ir interactions) successfully compete in energy with the agostic interaction. Fluorobenzene (PhF) was found to be a much better noncoordinating polar solvent for synthesis of the *t*-Bu complex than dichloromethane.

Metalloenzyme active sites have a variety of functional groups close to the metal binding site that modulate the reactivity of the metal site in interesting ways. For example, the distal histidine of hemoglobin is believed to affect the relative affinity of the metal binding site for CO versus O_2.[1]

We have attempted to apply these ideas to organometallic systems. The ready cyclometalation of 7,8-benzoquinoline has allowed access to a series of species of type **1**, where a labile site (X in **1a**; L′ in **1b**) is located very close to a pendant group G. The aim has been to see how the presence of G affects binding, structure, and reactivity at the labile site. We have described a number of applications of pendant amino groups (**1**, G = NH_2). For example, in **1a** (G = NH_2; X = F), protonation gives an HF complex (**1b**, G = NH_2; L′ = FH.) stabilized by F−H···N hydrogen bonding between the bound HF and G.[2a] When G = NH_2 and L′ is H_2 in **1b**, we see reversible proton transfer from coordinated H_2 to G.[2b]

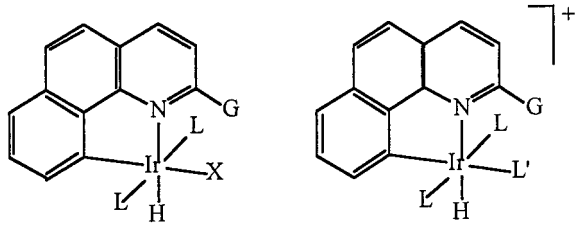

(L = PPh_3) **1a** **1b**

Turning to the case of G = *i*-Pr and *t*-Bu, we now report the effects of these large G groups on the properties of **1b**. The L′ binding site in **1b** now has a low affinity for external ligands, and for the G = *t*-Bu case, the product is an agostic compound with a CH bond of the *t*-Bu ligand coordinated to the sixth site. For G = *i*-Pr, in contrast, the potentially agostic *i*-Pr methyl groups point away from the metal, and evidence discussed here shows this species is nonagostic.

Agostic groups[3] are normally very common whenever a vacant coordination site in a complex is located in the vicinity of a nearby sp^3 or sp^2 C−H bond, so the failure of the isopropyl to become agostic in a system where the corresponding *tert*-butyl is agostic attracted our attention. The influence of the carbon skeleton on the choice of being agostic has already been noted.[4] In these earlier systems the observed agostic interaction was shown to be the result of a subtle balance between an attraction between the CH bond and the electron-deficient metal and repulsions between various groups within the ligands. Hybrid QM/MM methods have proved to be very efficient in describing such situations.[5] In this work ONIOM (B3PW91/UFF) calculations have been carried out to find the origin of the different behavior in the two groups: G = *i*-Pr vs *t*-Bu.

Results and Discussion

Synthesis of Ligands and Complexes 2 and 3. Benzoquinoline readily undergoes nucleophilic attack

* Corresponding authors. E-mail: odile.eisenstein@lsd.univ-montp2.fr (O.E.); robert.crabtree@yale.edu (R.H.C.); jack.faller@yale.edu (J.W.F.).
† Université Montpellier 2.
‡ Yale University.

(1) Collman, J. P.; Fu, L. *Acc. Chem. Res.* **1999**, *32*, 455.
(2) (a) Clot, E.; Eisenstein O.; Crabtree, R. H. *New J. Chem.* **2001**, *25*, 66. (b) Patel, B.; Lee, D.-H.; Rheingold A. L.; Crabtree, R. H. *Organometallics* **1999**, *18*, 1615. Lee, D.-H.; Patel, B. P.; Clot, E.; Eisenstein O.; Crabtree, R. H. *Chem. Commun.* **1999**, 297.
(3) Brookhart, M.; Green, M. L. H. *J. Organomet. Chem.* **1983**, *250*, 395. Brookhart, M.; Green, M. L. H.; Wong, L. L. Prog *Inorg. Chem.* **1988**, *36*, 6: 1. Crabtree, R. H. *Angew. Chem., Int. Ed. Engl.* **1993**, *32*, 789.
(4) Cooper, A. C.; Clot, E.; Huffman, J. C.; Streib, W. E.; Maseras, F.; Eisenstein, O.; Caulton, K. G. *J. Am. Chem. Soc.* **1999**, *121*, 97. Jaffart, J.; Etienne, M.; Maseras, F.; McGrady, J. E.; Eisenstein, O. *J. Am. Chem. Soc.* **2001**, *123*, 6000.
(5) Maseras, F. *Chem. Commun.* **2000**, 1821.

10.1021/om010802i CCC: $22.00
Publication on Web 01/10/2002

Table 1. Crystallographic Data for 2 and 3

	2	3
formula	$C_{53}H_{47}Cl_2F_6IrNP_3$	$C_{53}H_{47}Cl_2F_6IrNP_3$
fw	1168.00	1038.93
a, Å	20.3262(4)	11.1421(1)
b, Å	15.3816(3)	11.4068(3)
c, Å	15.2066(3)	17.9943(6)
α (deg)	90	80.692(2)
β (deg)	90	81.153(2)
γ (deg)	90	79.941(2)
V, Å^3	4754.3(1)	2203.6(1)
Z	4	2
cryst syst	orthorhombic	triclinic
space group	*Pnma* (#62)	*P*1 bar (No. 2)
ρ_{calcd}, g cm^{-3}	1.632	1.566
μ (Mo Kα) cm^{-1}	30.91	31.66
temperature, °C	−90	−90
λ (Å)	0.71069	0.71069
$R(F_o)$	0.031	0.033
$R_w(F_o)$	0.036	0.029
GOF	1.08	1.34

at the 2-position as a result of the polarization of the ring CN multiple bond; the *N*-oxide shows even greater reactivity. We have synthesized the new species bq-(*i*-Pr) and bq-(*t*-Bu) from the alkyl Grignard reagents and the benzoquinoline *N*-oxide by a known method.[6]

Cyclometalation of 2-substituted benzoquinolines with $[IrH_2L_2(H_2O)_2]PF_6$ normally affords an aqua complex (**1b**, L′ = H_2O), the water coming from the moist CH_2Cl_2 solvent. With the bulky substituted benzoquinolines used here, in contrast, the products were $[IrH(bq\text{-}R)L_2]PF_6$ (**2**, R = *i*-Pr; **3**, R = *t*-Bu), lacking an aqua group or any other external ligand.

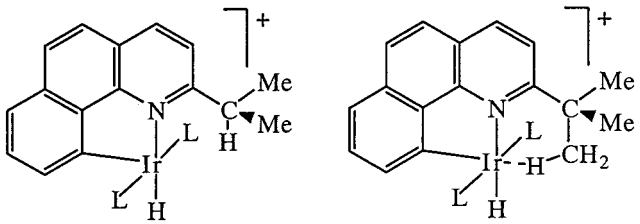

2 (R = i-Pr) **3** (R = t-Bu)

Unexpectedly, for bq-*t*-Bu, the cyclometalation gave very little product using the usual CH_2Cl_2 solvent. Moving to PhF—rarely encountered as a reaction solvent—gave a satisfactory yield. PhF is both less coordinating and less oxidizing than CH_2Cl_2, while still being polar enough to dissolve salts such as **3**.

Structures of Complexes 2 and 3. X-ray crystallographic study of the two species (Tables 1 and 2; Figures 1 and 2) showed that the *t*-Bu is agostic, as one might expect, whereas the isopropyl is not. The *t*-Bu complex (**3**) has one of its methyl groups pointing directly toward the metal and one of the hydrogen atoms of this methyl is clearly bound to the sixth site at iridium, as is typical in agostic complexes. All hydrogen atoms in the molecule were found in the difference Fourier and were refined. Although positions found by X-ray determinations are not particularly accurate, refining all hydrogens provides an internal calibration of the variations and errors in observed C−H distances. Even without this X-ray evidence for hydrogen positions, the location of the carbon of the methyl at 2.722(4) Å from Ir is entirely typical of an agostic system. NMR evidence, discussed below, confirms the assignment.

The isopropyl group of **2** is directed so the secondary CH, rather than the primary CH's, is pointing toward the metal. The observed Ir···H distance of 2.77 Å is considered too long for an agostic interaction, and **2** is therefore identified as a five-coordinate square pyramidal species. As the hydrogen atoms are not located well by X-ray crystallography and C−H distances appear shorter (∼0.95 Å) than the true distance (∼1.10 Å), a more realistic assessment of distances can be made by calculating an ideal position of the H based on the carbon positions. In a later section we discuss a computational study that locates this hydrogen more securely in a very similar position. The X-ray method tends to underestimate C−H distances, and so in agostic systems it tends to overestimate Ir···H distances. Regardless, none of the computations suggest an agostic interaction. The only ligand that might have escaped crystallographic detection would be a coordinated H_2, but the NMR spectroscopic study would certainly have detected this ligand.

In all other respects both structures are entirely conventional with no unusual intra- or intermolecular contacts. A conclusion that **2** is more stable in the nonagostic form would not be completely justified on the basis of X-ray data because two tautomers could be in equilibrium in solution and the least stable might have crystallized. For this reason, we have examined the NMR spectroscopic data.

Spectroscopy of 2 and 3. The case of **2** is the simplest. The NMR spectrum shows the terminal hydride as a triplet ($^2J_{HP}$ = 14.5 Hz.) at *δ* −12.47. There is no other high-field hydride or dihydrogen resonance visible in the temperature range used (20 to −80 °C). The isopropyl group appears as an intense (6H) doublet at *δ* 0.64 ($^3J_{HH}$ = 8.78 Hz), assigned to the isopropyl CH_3 group, and a multiplet of unit intensity at *δ* 2.67 and assigned to the isopropyl secondary CH. No significant change is seen in the temperature range mentioned. The IR spectrum shows the Ir−H stretch at 2184 cm^{-1}. Both the NMR and IR data are consistent with a nonagostic structure because the chemical shift of the *i*-Pr CH proton and the *ν*(CH) IR bands are normal; in particular there is no sign of agostic *ν*(CH) bands at low energy. Using a scaling between calculated ONIOM frequencies and experimental values of 0.9205, we predict an Ir−H stretching frequency for the agostic isomer for G = *i*-Pr at 2173 cm^{-1} and an agostic C−H stretch at 2549 cm^{-1}. While the *ν*(Ir−H) is found close to that predicted, the more important *ν*(C−H) is not seen in the predicted region, either in the crystal or in solution, consistent with the absence of the agostic tautomer in the experimental case.

For **3**, the NMR spectrum again shows the terminal hydride as a triplet ($^2J_{HP}$ = 14.7 Hz) but now at *δ* −14.34. Again, there is no high-field hydride or dihydrogen resonance visible in the temperature range used. At room temperature, the *tert*-butyl methyl groups appear as a singlet at *δ* 0.63. On cooling there is a decoalescence into a pair of singlets at *δ* 0.73 and −0.06 in a 2:1 intensity ratio that clearly correspond to agostic and terminal methyl groups of the *tert*-butyl. Line shape

(6) Cappelli, A.; Anzini, M.; Vomero, S.; Mennuni, L.; Makovec, F.; Doucet, E.; Hamon, M.; Bruni, G.; Romeo, M. R.; Menziani, M. C.; De Benedetti, P. G.; Langer, T. *J. Med. Chem.* **1998**, *41*, 728−741.

Table 2. Metric Data for the Structures Discussed[a]

	2x	2q	2m	2′q	2′m	3x	3q	3m
Ir···H(nonag)	2.77(6)	2.648	2.731					
Ir···C(nonag)	3.454(8)	3.438	3.500					
Ir···H(ag)				2.015	2.030	1.98(3)	2.062	2.073
Ir···C(ag)				2.741	2.853	2.722(4)	2.781	2.864
Ir−H(hydr)	1.49(8)	1.591	1.578	1.622	1.579	1.56(4)	1.605	1.578
Ir−N(bq)	2.154(6)	2.186	2.204	1.946	2.168	2.124(3)	2.145	2.178
Ir−C(bq)	1.981(7)	2.003	2.005	2.040	2.015	2.004(3)	2.017	2.008
Ir−P	2.324(1)	2.323	2.361	2.323	2.379	2.335(1)	2.319	2.110
Ir−P′	2.324(1)	2.323	2.362	2.322	2.348	2.334(1)	2.323	2.348
CH···HIr	2.16(7)	2.908	2.139	2.912	2.100	2.12(5)	2.967	2.384
C′H′···HIr	2.16(7)	2.956	2.142	3.189	2.358	2.46(5)	3.057	2.353
Ar···Ar′	4.02(3)		3.637		3.674	3.77(3)		3.67
Ar···Ar″	4.02(3)		3.705		4.903	4.43(3)		5.02
C−H(ag)				1.131	1.122	1.05(4)	1.131	1.120
N−C(α)−C(β)	118.3(6)	117.6	118.9	118.0	120.0	120.0(3)	119.4	121.4

[a] **2**, nonagostic *i*-Pr; **2′**, agostic *i*-Pr; **3**, agostic *tert*-butyl; **x**, experimental; **q**, quantum only; **m**, QM/MM; bq = benzoquinolinato; ag = agostic; hydr = hydride; Ar = arene centroid bq B ring; Ar′, Ar″ = Ph centroids PPh_3 B rings.

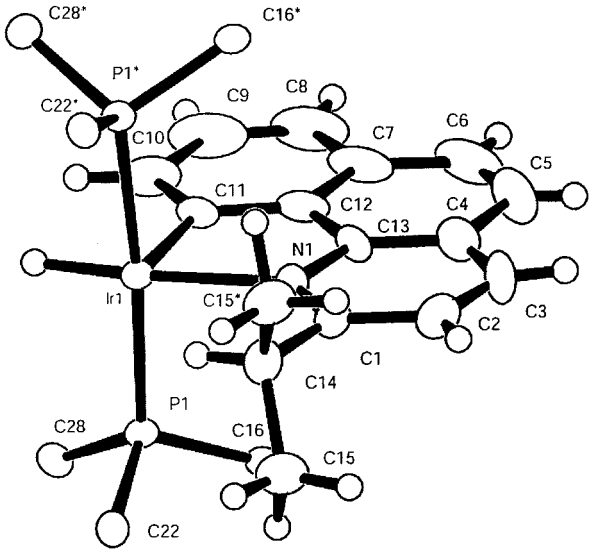

Figure 1. ORTEP diagram of the cation in [IrBq-*i*-Pr-$(PPh_3)_2$H]PF_6·CH_2Cl_2, **2**, showing 50% probability ellipsoids.

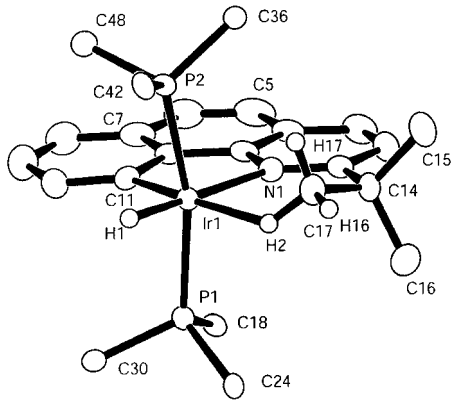

Figure 2. ORTEP diagram of the cation in [IrBq-*t*-Bu-$(PPh_3)_2$H]BF_4, **3**, showing 50% probability ellipsoids.

analysis gives an exchange barrier of 9.7 kcal/mol. This exchange process—a 1,3 shift of the metal from one methyl group to the other—can be frozen out but the protons of the agostic Me group remain a single sharp peak to −90° so the corresponding 1,1′ agostic shift—exchanging the metal between geminal CH bonds of a single CH_3 group—is much easier. We have reported this order of barriers in studies of Ir(I) alkane species, intermediates in H/D exchange reactions, where the barriers were predicted to be 11.7 (1,3) and 2.5 (1,1′) kcal/mol, respectively; in the first case, this is close to the 1,3 barrier found here.[7] We ascribed the low 1,1′ barrier height to the metal remaining bound to the same carbon throughout in the 1,1′ process but having to shift from one carbon to another in the 1,3 process and so losing most of the M···alkyl binding energy in the transition state.

Computational Study

In what follows, **2x** refers to the experimental values, **2q** to the pure quantum studies, and **2m** to the QM/MM calculations; metric data are defined in the same way. The same labeling is used for the *tert*-butyl complex, **3**.

The fact that the isopropyl complex, **2x**, is nonagostic when it could apparently have become agostic was a puzzle that led us to carry out computational work to try to identify the factors involved. Calculations were carried out using pure quantum mechanical (QM) methods (DFT, B3PW91) using the model compound **2q** having PH_3 ligands. In the *i*-Pr case, both agostic and nonagostic situations could be modeled starting from the *i*-Pr crystal structure for the nonagostic situation and starting from the *t*-Bu crystal structure for the agostic case, but replacing one terminal methyl of the *t*-Bu group by H. Previous calculations have proved capable of predicting agostic or nonagostic character in such cases and have identified the factors that control the outcome.[4,5]

The optimized nonagostic structure (**2q**) so obtained closely fits the experimental one (**2x**, Figure 1), as shown by the comparison data of Table 2. The hydrogen that lies closest to the metal, also present in the experimental structure, is probably better located by the computational work than by the X-ray method. The Ir···H distance is 2.648 Å, and the CH distance is 1.106 Å. This is very different from the usual agostic situation, and the CH bond pointing toward the metal is not significantly elongated compared to the most appropriate reference value of 1.102 Å calculated for the corresponding unambiguously unbound secondary CH bond in the agostic tautomer. This work confirms that the *i*-Pr compound is genuinely nonagostic and five-coordinate.

(7) Gérard, H.; Eisenstein, O.; Lee, D−H.; Chen, J.; Crabtree, R. H. *New J. Chem.* **2001**, *25*, 1121.

Table 3. Comparison of Relative Calculated Energies for Agostic 2′q vs Nonagostic 2q[a]

compound	QM (kcal/mol)	QM/MM (kcal/mol)	QM part of QM/MM (kcal/mol)
2′q (agostic)	−0.7	0.0	0.0
2q (nonagostic)	0.0	−3.2	−0.2

[a] Most stable isomer indicated by negative sign in each case.

This information gives some insight into why an aqua complex is not formed for **2**. The *i*-Pr secondary CH hydrogen being 2.65 Å (calcd) from the Ir prevents the water from binding because a typical Ir−OH_2 distance range is 2.2−2.4 Å, which would put the water oxygen far too close (<1 Å) to this H. This steric effect excludes water from the site.

The bound primary CH of the −CH(CH_3)$_2$ group in the calculated agostic tautomer, **2′q**, has an elongated C−H distance of 1.131 Å and a short Ir···C distance of 2.777 Å, entirely in accord with the normal situation found for true agostic structures. The shorter Ir−N distance in the agostic (2.137 Å) versus the nonagostic (2.186 Å) isomer is consistent with the presence of an attractive Ir···HC interaction in the agostic structure. The agostic carbon is not in the bq plane and on the opposite side of the bq plane from the agostic H; this is probably the result of the C−H bond, rather than the CH hydrogen, being the true ligand.[8] The Ir−N bond is readily distorted in the sense that its length varies considerably both in experimental and calculated structures in this series of compounds.[2] This is probably due to an intrinsically weaker bonding of a pyridine versus, for example, the bq aryl, but also may be a result of the high trans influence hydride weakening this bond. Any attractive Ir···HC interaction would be expected to cause the bq ligand to tilt in such a way as to bring the CH closer to the metal. Given the relative inflexibility of the bq Ir−C(aryl) bond, the more flexible Ir−N bond might be expected to shorten, as indeed is observed. The bq ligand itself is relatively rigid, as shown by the very small changes in the bond angles, for example in the N_α−C_β−C_γ angle (see diagram **2q**).

The energy difference between the two tautomers, **2q** and **2′q**, at this level of calculation is 0.7 kcal/mol in favor of the agostic tautomer, **2′q**, a value that is in reasonable agreement with experiment considering the errors possible in such calculations (Table 3).

We decided to undertake a combined quantum mechanical/molecular mechanics calculation to take into account the steric effects of the phenyl groups in the real PPh_3 ligands. This was done via the ONIOM method (see Computational Details). The agostic and nonagostic tautomers were once again optimized, resulting in the metric parameters shown in Table 2. The increased steric bulk of the phosphine on going from pure QM (**2q**) to QM/MM (**2m**, ONIOM(B3PW91/UFF)) has the expected effect of causing the *i*-Pr group to recede slightly from the metal. The agostic CH bond moves slightly away from the metal and shortens slightly relative to the pure QM case, as can be seen by comparing the metric data in Table 2. The energy difference between the two tautomers at this level of calculation is 3.2 kcal/mol in favor of the nonagostic tautomer. This is fully consistent with the NMR and IR spectroscopic observations suggesting that the nonagostic tautomer is present in solution, as well as with the X-ray structure.

Analysis of the QM and MM contributions to the total energy in the QM/MM calculations shows that the QM energies are identical (within 0.2 kcal mol^{-1}) for the two isomers. Thus the small energetic preference for the agostic isomer found in the pure QM calculations has been lost. This means the preference for the nonagostic isomer has to come from the MM contribution.

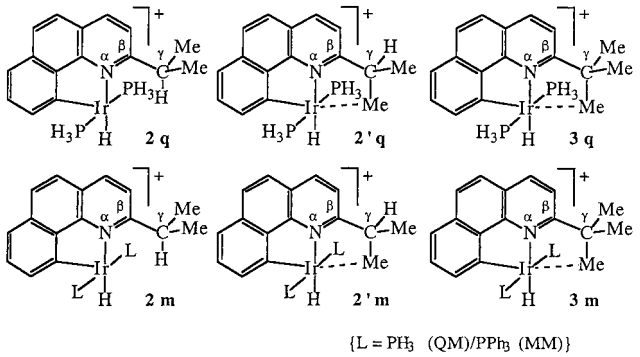

PPh_3/bq, CH···HIr, and CH···Ir Interactions in Complexes 2 and 3. Close examination of the structures of **2** and **3** suggests that the agostic interaction is just one of a number of structural motifs that are expected to affect the energetics of the system. These motifs seem to have competitive energy contributions, and the agostic interaction is obviously not dominant since the nonagostic structure is preferred for **2**. The Ir···HC geometry will not be described further since it is similar to that in the QM work.

One such contribution is aromatic parallel (||) stacking between a P−Ph substituent and the benzoquinoline. Because of the cis arrangement of PPh_3 and bq groups and the pyramidality at P, the stacking cannot be perfectly parallel; the experimental dihedral angle is close to 20°, the minimum achievable without strain. We will call the pyridine ring of the benzoquinoline the A ring, the central bq ring the B ring, and the cyclometalated benzo ring the C ring. Of the three, only the B ring is far enough away from the metal to participate in significant || stacking interactions with a cis PPh_3 group. Although such effects have been relatively little discussed in the literature,[9] they may be generally important in metal complexes. Another potential attractive interaction, perpendicular (⊥) stacking, does not seem to be important in this structure.

For the *t*-Bu (**3**) compound, both the experimental (**3x**) and the QM/MM structure (**3m**, Figure 3) show there is one aromatic stacking interaction between the bq B ring and one Ph group (ring B′) of one PPh_3 ligand. The centroid−centroid distances from the Ph ring to the bq B ring are 3.67 Å (B′) and 5.02 Å (B″) (**3m**) versus 3.57 Å (B′) and 5.48 Å (B″) (**3x**, Figure 2). In contrast, for **2**, the agostic structure (**2′m**, Figure 4) also has one such interaction, but the observed nonagostic structure (**2x**

(8) Crabtree, R. H.; Holt, E. M.; Lavin, M.; Morehouse, S. M. *Inorg. Chem.* **1985**, *24*, 1986.

(9) Munakata, M.; Ning, G. L.; Suenaga, Y.; Kuroda-Sowa, T.; Maekawa, M.; Ohta, T. *Angew. Chem., Int. Ed.* **2000**, *39*, 4555. Ezuhara, T.; Endo, K.; Matsuda, K.; Aoyama, Y. *New J. Chem.* **2000**, *24*, 609. Scudder, M. L.; Goodwin, H. A.; Dance, I. G. *New J. Chem.* **1999**, *23*, 695−705. Cundari, T. Personal communication, 2001.

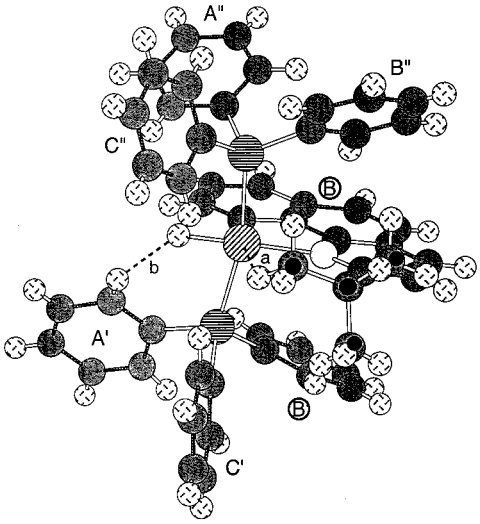

Figure 3. Diagram of the QM/MM calculated structure (ONIOM(B3PW91/UFF)) of the agostic *tert*-butyl, **3m**. The G group is marked with solid spheres. The π-stacked rings are identified with an open circle around their labels. CH···HM contacts are dotted and marked 'b'. The CH···M interaction is dotted and marked 'a'.

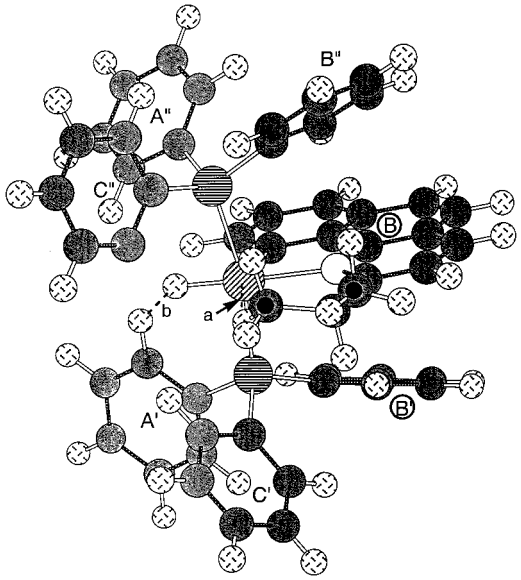

Figure 4. Diagram of the QM/MM calculated structure (ONIOM(B3PW91/UFF)) of the agostic isopropyl, **2′m**. The G group is marked with solid spheres. The π-stacked rings are identified with an open circle around their labels. CH···HM contacts are dotted and marked 'b'. The CH···M interaction is dotted and marked 'a'. One aryl H has been removed to avoid obsuring key parts of the diagram.

and **2m**) has two, one on one side of the bq B ring and the other on the other side. This is shown from the centroid−centroid distances from the PPh_3 B′ and B″ ring to the bq B ring of 3.637 and 3.705 Å (**2m**, Figure 5), versus 3.765 Å (twice) (**2x**), entirely appropriate for face-to-face stacking. In the agostic structure **2′m** one Ph ring (B′) remains within stacking distance (3.674 Å) of the B ring, but the other (B″) moves away (4.903 Å). The loss of one favorable || aromatic stacking interaction on going from the nonagostic to the agostic structure could therefore be a factor that favors the observed structure.

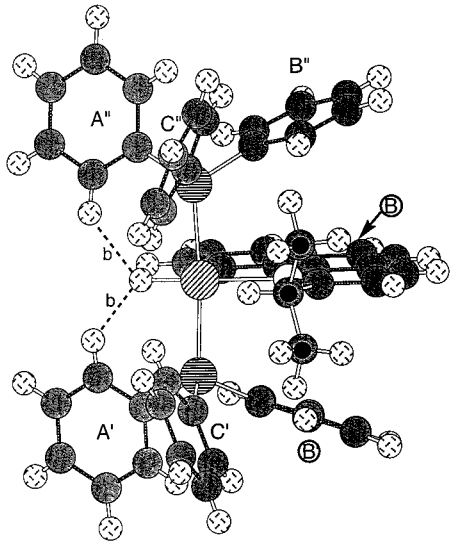

Figure 5. Diagram of the QM/MM calculated structure (ONIOM(B3PW91/UFF)) of the nonagostic isopropyl, **2m**. The G group is marked with solid spheres. The π-stacked rings are identified with an open circle around their labels. CH···HM contacts are dotted and marked 'b'.

In line with the above argument, the PPh_3 ligands are almost perfectly eclipsed in nonagostic **2x**, where B′···B···B″ stacking occurs, but are staggered in agostic **3x** and **2′m**, where only B′···B stacking is present.

The *t*-Bu (**3m**) compound also contains one C−H···H−Ir motif in which an ortho-CH bond of a PPh_3 phenyl group points toward the metal hydride with the result that the H···H nonbonding distance is 2.110 Å (ONIOM); the experimental situation is very similar, but the H's are less well located by X-ray and X−H bonds are subject to systematic shortening. We have previously drawn attention to the fact that C−H···H−M interactions are quite common in the structures of transition metal hydride complexes in general.[10] In this prior work we emphasized cases where the H positions were determined by neutron diffraction to avoid systematic errors associated with X-ray data.

For **2m**, there are two CH···HM interactions in the nonagostic case, with *d*(H···H) of 2.142 and 2.139 Å (ONIOM); the experimental structure **2x** shows a very similar arrangement, but the H's are not well located. On going to the agostic structure, **2′m**, these change to 2.099 and 2.358 Å, meaning that only one of the two original CH···HM interactions is still present. Once again, we have a factor that could destabilize the agostic form and account for its being less stable.

The P−Ir−P angle increases significantly on going from the agostic to the nonagostic structures: P−Ir−P is 159° in the agostic tBu (**3m**), 166° in the agostic *i*-Pr (**2′m**), and 174° in the nonagostic *i*-Pr (**2m**). An increase in the number of $\pi-\pi$ stacking interactions—favored by more ideally trans phosphines—causes the phosphine ligands to move away from the unhindered hydride and toward the bq to maximize the $\pi-\pi$ attractions in **2m**, as also shown by the trend in H−Ir−P angles: 80.5° in agostic **3m**, 80° in agostic **2′m**, and 87.3° in nonagostic **2m**.

(10) Richardson, T.; Koetzle, T. F.; Crabtree, R. H. *Inorg. Chim. Acta* **1996**, *250*, 69.

Thus we see three main types of interactions at work in these structures: || aromatic stacking, C−H···H−Ir interactions, and an agostic C−H···Ir. Each seems to have broadly similar energy contributions, and thus no one interaction is dominant. The agostic interaction may therefore fail to occur when this leads to the loss of other favorable interactions.

Conclusions

Agostic interactions are not always dominant in determining structure but compete with other weak interactions such as those between ligands. Here, we report a case where the agostic tautomer is disfavored. The resulting vacancy at the metal is stabilized by the high trans effect bq aryl ligand in the trans position. Ligand−ligand interactions, in this case π-stacking, can dominate and prevent the agostic interaction.

Computational Details

All calculations were performed with the Gaussian 98 set of programs[11] with the ONIOM method.[12] The complexes Ir(H)(bq-G)$(PPh_3)_2^+$ (**2m**, G = *i*-Pr; **3m**, G = tBu) were optimized at the ONIOM(B3PW91/UFF) level,[13] where the QM part was Ir(H)(bq-G)$(PH_3)_2^+$. The G group was explicitly included in the QM part. The iridium atom was represented by the relativistic effective core potential (RECP) from the Stuttgart group (17 valence electrons) and its associated (8s7p5d)/[6s5p3d] basis set,[14] augmented with an f function ($\alpha = 0.95$). The phosphorus atoms were also treated with Stuttgart's RECPs and the associated basis set,[15] augmented by a polarization d function ($\alpha = 0.387$). A 6-31G(d,p) basis set[16] was used for the hydrides and for both nitrogen atoms. The remaining atoms were treated by a 6-31G basis set. The molecular mechanics calculations were performed with the UFF force field.[17] The model systems Ir(H)(bq-G)$(PH_3)_2^+$ (**2q**, G = *i*-Pr; **3q**, G = *t*-Bu) were also optimized at the B3PW91 level in pure QM calculations. The nature of the extrema (ONIOM(B3PW91/UFF) and QM(B3PW91)) was checked through analytical computation of the vibrational frequencies.

Experimental Details

2-Isopropyl-7,8-benzoquinoline. A solution of 7,8-benzoquinoline *N*-oxide[6] (2.06 g, 10.55 mmol) in 40 mL of anhydrous THF was cooled to 0 °C. Subsequent treatment with *i*-PrMgCl (2.0 M solution in diethyl ether, 15.3 mL in 20 mL of THF) over a 10 min period resulted in a color change to opaque brown. After stirring at room temperature under Ar for 4 h, the reaction mixture was poured into 10% aqueous NH_4Br (100 mL) and extracted with $CHCl_3$ (3 × 40 mL). The combined extracts were dried over Na_2SO_4 and treated overnight with MnO_2 (65 g). The filtered chloroform solution was evaporated to dryness, and the residue was chromatographed on a silica column using benzene as the eluent to yield 1.4 g (60%) of yellow oil, which partially crystallized on standing. Anal. Calcd for $C_{16}H_{15}N\cdot 0.2H_2O$: C, 85.50; H, 6.85; N, 6.23. Found: C, 85.45; H, 6.62; N, 6.24. ^{1}H NMR (C_6D_6, 500 MHz): 9.77 (d, *J*H−H = 8.5, 1H), 7.30−7.60 (m, 4H), 7.23 (d, *J*H−H = 9.6, 1H), 7.15 (s, 1H), 6.93 (d, *J*H−H = 9.6, 1H), 3.17 (m, 1H), 1.42 (d, *J*H−H = 8.5, 6H).

2-*tert*-Butyl-7,8-benzoquinoline was obtained as a pale yellow solid via the method described above under Ar but using *t*-BuMgCl and CH_2Cl_2 as the eluent. Yield = 50%, 1.24 g. Anal. Calcd for $C_{17}H_{17}N\cdot 0.1H_2O$: C, 86.15; H, 7.25; N, 5.90. Found: C, 86.02; H, 6.97; N, 5.33. ^{1}H NMR (C_6D_6, 500 MHz): 9.68 (d, *J*H−H = 8.3, 1H), 7.20−7.60 (m, 6H), 7.12 (s, 1H), 1.47 (s, 9H).

2-Isopropyl-7,8-benzoquinolato(hydrido)bis(triphenylphosphine)iridium (III) Hexafluorophosphate (2). $[Ir(H)_2(PPh_3)_2(H_2O)_2][PF_6]$ (500 mg, 0.556 mmol) was dissolved in degassed, moist CH_2Cl_2 (20 mL) under Ar and cooled to 0 °C. A solution of 2-isopropyl-7,8-benzoquinoline (123 mg, 0.556 mmol) in 10 mL of CH_2Cl_2 was added dropwise over 10 min. The resulting pale orange solution was allowed to stir at room temperature for 1 h. The solution was concentrated to 20 mL, and 20 mL of anhydrous diethyl ether was added as an upper layer. Orange crystals of the product accumulated upon standing overnight at room temperature. Yield: 57%, 343 mg. Anal. Calcd for $C_{52}H_{45}F_6IrNP_3\cdot CH_2Cl_2$: C, 59.32; H, 4.38; N, 1.30. Found: C, 59.12; H, 4.56; N, 1.33. IR (KBr, cm^{-1}): 2184 (νIr−H). ^{1}H NMR (CD_2Cl_2, 500 MHz): −12.47 (t, ^2JH−P = 14.50, 1H, Ir−H), 0.64 (d, *J*H−H = 8.78, 6H, CH_3), 2.67 (m, 1H, MeCH), 6.7−7.4 (m, 36H, arom.), 8.07 (s, 1H). ^{31}P{^{1}H} NMR (CD_2Cl_2, 202.4 MHz): 25.45 (s).

2-*tert*-Butyl-7,8-benzoquinolato(hydrido)bis(triphenylphosphine)iridium (III) Tetrafluoroborate (3). A suspension of $[Ir(H)_2(PPh_3)_2(H_2O)_2][BF_4]$ (400 mg, 0.486 mmol) in degassed fluorobenzene (30 mL) was cooled under Ar to 0 °C. A solution of 2-*tert*-butyl-7,8-benzoquinoline (114 mg, 0.486 mmol) in fluorobenzene (10 mL) was added dropwise over 30 min, and the resulting mixture was stirred at room temperature for 18 h. Addition of moist pentane (20 mL) resulted in the precipitation of an off-white solid, which was collected and recrystallized from CH_2Cl_2/pentane (1:1) to give the product as colorless crystals. Yield: 30%, 151 mg. Anal. Calcd for $C_{53}H_{47}F_4IrNBP_2$: C, 61.27; H, 4.52; N, 1.34. Found: C, 61.14; H, 4.49; N, 1.39. IR (KBr, cm^{-1}): 2166 (νIr−H), 2479, 2572 (agostic Ir−CH_3). ^{1}H NMR (CD_2Cl_2, 500 MHz): −14.34 (t, ^2JH−P = 14.67, 1H, Ir−H), 0.63 (s, 9H, CH_3), 6.49 (d, *J*H−H = 7.90, 1H), 6.62 (t, *J*H−H = 8.20), 7.10−7.50 (m, 34H), 8.15 (d, *J*H−H = 8.57, 1H). ^{31}P{^{1}H} NMR (CD_2Cl_2, 202.4 MHz): 20.41 (s). The PF_6 salt was obtained in the same way in similar yield starting from the appropriate bis-aqua PF_6 salt.

Crystallographic Details. Single crystals of **2** and **3** suitable for X-ray analysis were formed upon standing from a methylene chloride/diethyl ether or a methylene chloride/pentane solution, respectively. Crystallographic data are summarized in Table 1. The structures were determined from data collected with a Nonius KappaCCD diffractometer at −90 °C. Lorentz and polarization corrections were applied to all data. The structures were solved by direct methods (SIR92) using the teXan crystal structure analysis package, and the function minimized was $\sum w(|F_o| - |F_c|)^2$ in all cases. Hydrogen atoms were located in the difference maps and were refined. Compound **2** crystallized in the space group *Pnma*, and the iridium, as well as many ligand atoms, lie on special positions in a mirror plane; hence the cation has a plane of symmetry through the Bq ligand.

Acknowledgment. We thank the NSF for funding.

OM010802I

(11) Frisch, M. J.; Trucks, G. W.; Schlegel, H. B.; Scuseria, G. E.; Robb, M. A.; Cheeseman, J. R.; Zakrzewski, V. G.; Montgomery, J. A.; Stratmann, R. E.; Burant, J. C.; Dapprich, S.; Millam, J. M.; Daniels, A. D.; Kudin, K. N.; Strain, M. C.; Farkas, O.; Tomasi, J.; Barone, V.; Cossi, M.; Cammi, R.; Mennucci, B.; Pomelli, C.; Adamo, C.; Clifford, S.; Ochterski, J.; Petersson, G. A.; Ayala, P. Y.; Cui, Q.; Morokuma, K.; Malick, D. K.; Rabuck, A. D.; Raghavachari, K.; Foresman, J. B.; Cioslowski, J.; Ortiz, J. V.; Stefanov, B. B.; Liu, G.; Liashenko, A.; Piskorz, Komaromi, P. I.; Gomperts, G.; Martin, R. L.; Fox, D. J.; Keith, T.; Al-Laham, M. A.; Peng, C. Y.; Nanayakkara, A.; Gonzalez, C.; Challacombe, M.; Gill, P. M. W.; Johnson, B. G.; Chen, W.; Wong, M. W.; Andres, J. L.; Head-Gordon, M.; Replogle, E. S.; J. A. Pople J. A. *Gaussian 98*; Gaussian, Inc.: Pittsburgh, PA, 1998.

(12) Svensson, M.; Humbel, S.; Froese, R. D. J.; Matsubara, T.; Sieber, S.; Morokuma, K. *J. Phys. Chem.* **1996**, *100*, 19357.

(13) (a) Becke, A. D. *J. Chem. Phys.* **1993**, *98*, 5648. (b) Perdew, J. P.; Wang, Y. *Phys. Rev. B* **1992**, *82*, 284.

(14) Andrae, D.; Häussermann, U.; Dolg, M.; Stoll, H.; Preuss, H. *Theor. Chim. Acta* **1990**, *77*, 123.

(15) Bergner, A.; Dolg, M.; Küchle, W.; Stoll, H.; Preuss, H. *Mol. Phys.* **1990**, *30*, 1431.

(16) Hariharan, P. C.; Pople, J. A. *Theor. Chim. Acta* **1973**, *28*, 213.

(17) Rappe, A. K.; Casewitt, C. J.; Colwell, K. S.; Goddard, W.; A.; Skiff, W. M. *J. Am. Chem. Soc.* **1992**, *114*, 10024.